



ORIGINAL ARTICLE

Synthesis and evaluation of 5-aminimidazole-4-carboxamide riboside derivatives as anti-fatigue agents



Huimin Zhu^a, Wanbo Zeng^a, Tangna Zhao^b, Weiguo Shi^a, Xiao Dong^b,
Aiping Zhang^b, Xiang Li^{c,*}, Liang Xu^{a,*}

^a State Key Laboratory of Toxicology and Medical Countermeasures, Beijing Institute of Pharmacology and Toxicology, Beijing, China

^b State College of Pharmacy, Shanxi Medical University, Taiyuan, China

^c State National Resource Center for Chinese Materia Medica, China Academy of Chinese Medical Sciences, Beijing, China

Received 26 July 2022; accepted 26 September 2022

Available online 29 September 2022

KEYWORDS

AICAR;
Derivative;
Fatigue;
AMPK

Abstract Fatigue has a negative influence on daily life and work, and serious or chronic fatigue can even cause health problems. Studies have shown that 5-aminoimidazole-4-carboxamide-1- β -D-ribofuranoside (AICAR) can exert anti-fatigue effects by activating AMP-activated protein kinase (AMPK). In this study, six AICAR derivatives with substitution at the hydroxyl sites of the ribose moiety were synthesized and evaluated as anti-fatigue agents. All of the derivatives were demonstrated to effectively resist fatigue in animal models. The mice treated with the optimal compound **ZHM-01** showed an 8.6-fold greater exhaustion distance in the running wheel test and a 5.1-fold greater exhaustion time in the weight-loaded swimming test than those of the blank control group. **ZHM-01** treatment also reduced lactic acid (LA) and blood urea nitrogen (BUN) accumulation during exercise. In addition, **ZHM-01** administration enhanced the phosphorylation of AMPK but did not excite the central nervous system. Moreover, **ZHM-01** showed good biological safety in a 21-day toxicity evaluation. This study provides a new reference for the development of treatments for fatigue-related health problems.

© 2022 The Author(s). Published by Elsevier B.V. on behalf of King Saud University. This is an open access article under the CC BY-NC-ND license (<http://creativecommons.org/licenses/by-nc-nd/4.0/>).

* Corresponding Author.

E-mail addresses: m18222616303@163.com (X. Li), wj24998@163.com (L. Xu).

Peer review under responsibility of King Saud University.



1. Introduction

Fatigue is usually described as an overall feeling of tiredness or the inability of muscles to maintain the required level of strength for exercise (Cui et al., 2020; Hu et al., 2020; Zhu et al., 2021b). Fatigue can cause various disorders of the bio-regulatory, autonomic nervous, endocrine, and immune systems, thus causing a threat to human health. Besides, many diseases (especially cancer) lead to lasting and debilitating fatigue, which has a profoundly negative effect on patient recovery (Li et al., 2021, Wang et al., 2021). So far, there are no clear recommendations to treat muscle fatigue. Many nutritional supplements (vitamin, nucleotide, amino acids, etc.) (Shimizu et al., 2010, Xu et al., 2017, Coqueiro et al., 2019), as well as bioactive ingredients in natural products (such as taurine, ginseng, curcumin, etc.) (Gao et al., 2018, Zheng et al., 2019, Kim et al., 2022), were reported with anti-fatigue effects and consequently improving exercise performances, however, these molecules always need to be dosed for several weeks to take effect. Besides, several pharmacological therapies, such as modafinil and caffeine, can also improve exercise performance, but their central stimulant often rise negative effects after long-term use, and the variety of anti-fatigue drugs are limited (Nakagawasai et al., 2021, Peng et al., 2021). Therefore, there is a great need to identify potential alternatives that have definite efficacy and fewer side effects (Chen et al., 2021).

AMPK is an important biomacromolecule that regulates biological energy metabolism (Luo et al., 2019; Norikura et al., 2020; Zhang et al., 2019b). It is expressed in various metabolism-related organs and can be activated by a range of stimuli, including ATP, cellular stress, exercise, oxidative stress, and substances that can affect cellular metabolism. AMPK agonists have been demonstrated to significantly relieve fatigue (Lin and Hardie 2018, Weihrauch and Handschin 2018). For example, arctigenin has AMPK excitatory activity and can increase the expression of antioxidation-related genes by regulating the AMPK/p53/nuclear factor erythroid 2-related factor 2 (Nrf2) and AMPK/peroxisome proliferator-activated receptor γ coactivator-1 α (PGC-1 α) pathways, which have been shown to resist the generation of exercise fatigue and to improve the exercise endurance of mice (Tang et al., 2011, Wu et al., 2014).

The adenosine analogue 5-aminoimidazole-4-carboxamide-1- β -D-ribofuranoside (AICAR, also known as acadesine) is involved in the anabolism of purine nucleotides in the human body (Yoon et al., 2019). AICAR has been demonstrated to have definite AMPK agonist activity, and a phase III clinical trial has shown that it can improve ischemic reperfusion injury after coronary artery bypass grafting (Scudiero et al., 2016). In addition, Narkar *et al.* found that AICAR treatment for 4 weeks enhanced running endurance by 44% in sedentary mice through gene reprogramming of the AMPK-peroxisome proliferator-activated receptor delta signaling pathway (Narkar et al., 2008). However, AICAR is very hydrophilic, can be rapidly metabolized, and has a low bioavailability. Moreover, its administration has been shown to cause side effects such as lactic acid (LA) and uric acid accumulation (Dixon et al., 1991, D'Errico et al., 2012). In this study, AICAR derivatives with modification at the hydroxyl sites of the sugar moiety were synthesized, which aimed to have an improved molecular lipophilicity and potency compared to the parent compound. The anti-fatigue effects of these derivatives were assessed by several experiments in mice. The optimal molecule was further evaluated for its possible mechanism and safety.

2. Materials and methods

2.1. Materials

The reagents, raw materials, and solvents used in the synthesis were obtained from Beijing InnoChem Science & Technology Co., Ltd. (Beijing, China). The LA and BUN determination

kits were obtained from Nanjing Jiancheng Bioengineering Institute Co., Ltd. (Nanjing, China). Dulbecco's modified Eagle's medium (DMEM) was purchased from Tianjin Bocheng Technology Co., Ltd. (Tianjin, China). Protein electrophoresis buffer was purchased from Sangon Biotech (Shanghai) Co., Ltd. (Shanghai, China). C2C12 myoblasts were obtained from Nanjing Kebai Biotechnology Co., Ltd. (Nanjing, China). Anti-AMPK, anti-phospho-AMPK (Thr172), and anti-PGC-1 α primary antibodies as well as horseradish peroxidase-conjugated IgG secondary antibodies (rabbit and mouse) were from Beijing ComWin Biotech Co., Ltd. (Beijing, China).

2.2. Synthesis and characterization

2.2.1. 2',3',5'-Tri-O-acetyl-inosine (2)

To a round-bottom flask containing magneton, inosine **1** (10.0 g, 0.0373 mol), anhydrous pyridine (100 mL), and propionic anhydride (11.2 mL, 0.117 mol) were added. The mixture was stirred at room temperature for 24 h. The solution was quenched with EtOH (5 mL) and then concentrated three times *in vacuo* with 100 mL of toluene. The obtained white solid was collected, washed with cold EtOH (4 °C, 50 mL), and dried *in vacuo* with phosphorus pentoxide at 40 °C to obtain **2**. Yield: 99.9%; ¹H NMR (400 MHz, DMSO *d*₆) δ _H 8.21 (s, 1H), 8.04 (s, 1H), 6.17 (d, *J* = 5.3 Hz, 1H), 5.88 (dd, *J* = 5.3, 5.2 Hz, 1H), 5.61 (dd, *J* = 5.2, 4.9 Hz, 1H), 4.42–4.50 (m, 2H), 4.38 (dd, *J* = 12.3, 4.5 Hz, 1H), 2.16 (s, 3H), 2.15 (s, 3H), 2.11 (s, 3H); MS (*m/z*) 395.35 [M + H]⁺.

2.2.2. 2',3',5'-Tri-O-acetyl-1-[(2-methoxyethoxy) methyl] inosine (3)

To the mixture of **2** (14.7 g, 0.0373 mol) and CH₂Cl₂ (262 mL) was added *i*-Pr₂NEt (9.73 mL) at 0 °C. The reaction mixture was treated with benzyl chloromethyl ether (5.12 mL) and stirred for 65 min. The reaction was quenched with H₂O, stirred for 20 min, and then diluted with CHCl₃. The aqueous layer was extracted with CHCl₃. The combined organic layers were washed with H₂O and then with saturated sodium chloride, dried (MgSO₄), and concentrated. The crude product was purified by column chromatography (EtOAc-MeOH, 50:1) to obtain **3**. Yield: 80%; ¹H NMR (400 MHz, DMSO *d*₆) δ _H 8.11 (s, 1H), 7.94 (s, 1H), 7.36–7.27 (m, 5H), 6.09 (d, *J* = 4.9 Hz, 1H), 5.85 (t, *J* = 5.4, 4.9 Hz, 1H), 5.60 (dd, *J* = 5.4 Hz, 1H), 5.59 (s, 2H), 4.68 (s, 2H), 4.45–4.42 (m, 2H), 4.37 (m, 1H), 2.15 (s, 3H), 2.13 (s, 3H), 2.11 (s, 3H); MS (*m/z*) 515.49 [M + H]⁺.

2.2.3. AICAR

To the mixture of intermediate **3** (13.43 g, 0.0183 mol) and MeOH (110 mL) was added aqueous NH₃ solution (28%, 57 mL). The reaction mixture was stirred at room temperature for 1 h and concentrated *in vacuo* to obtain the deprotected nucleoside. The crude product was used for the next alkaline hydrolysis without further purification. A stirred mixture of deprotected nucleoside and aqueous NaOH (0.2 M, 200 mL) was heated under reflux for 1 h. After cooling, the reaction mixture was neutralized with aqueous HCl (6 M) and then concentration *in vacuo*. The residue was extracted with hot EtOH, filtered, concentrated *in vacuo*, and purified by column chromatography (CHCl₃-MeOH, 3:1) to obtain AICAR.

Yield: 70%; ^1H NMR (400 MHz, DMSO d_6) δ_{H} 7.30 (s, 1H), 6.70 (br s, 2H), 5.91 (s, 2H), 5.45 (d, $J = 6.4$ Hz, 1H), 5.35 (d, $J = 6.4$ Hz, 1H), 5.22 (dd, $J = 5.2, 4.9$ Hz, 1H), 5.14 (d, $J = 4.6$ Hz, 1H), 4.28 (dd, $J = 6.3, 5.9$ Hz, 1H), 4.09 (m, 1H), 3.90 (m, 1H), 3.58 (m, 2H); MS (m/z) 259.11 [$\text{M} + \text{H}$] $^+$.

2.2.4. 2',3'-O-Isopropylidene-acadesine (ZHM-01)

To the mixed solution of AICAR (10 g, 0.0397 mol) and acetone (1500 mL) was added *p*-toluene sulfonic acid (31.25 g, 0.181 mol) and triethyl orthoformate (39 mL, 0.234 mol). The reaction mixture was stirred overnight at room temperature. After neutralization with saturated sodium bicarbonate solution, the solution was concentrated *in vacuo* and cooled for crystallization. After filtration and drying, ZHM-01 was obtained. Yield: 98.7%; ^1H NMR (400 MHz, DMSO d_6) δ_{H} 7.34 (s, 1H), 6.76 (m, 2H), 5.91 (s, 2H), 5.72 (d, $J = 3.0$ Hz, 1H), 5.27 (q, $J = 2.4$ Hz, 1H), 5.05 (dd, $J = 2.4$ Hz, 1H), 4.83 (dd, $J = 3.0$ Hz, 1H), 4.04 (m, 1H), 3.45 (m, 2H), 1.28 (s, 3H), 1.20 (s, 3H); MS (m/z) 299.13 [$\text{M} + \text{H}$] $^+$.

2.2.5. 2',3',5'-Tri-O-acetyl-acadesine (ZHM-02)

To the mixed solution of AICAR (1 g, 0.037 mol) and anhydrous pyridine (10 mL) was added acetic anhydride (1.12 mL). The reaction mixture was stirred 6 h at room temperature. The solution was quenched with EtOH (0.5 mL) and then concentrated three times *in vacuo* with 10 mL of toluene. The obtained white solid was collected, washed with cold EtOH (4 °C, 10 mL), concentrated *in vacuo*, and purified by column chromatography (ethyl acetate-petroleum ether, 1:2) to obtain ZHM-02. Yield: 82.6%; ^1H NMR (400 MHz, DMSO d_6) δ_{H} 7.40 (s, 1H), 5.88 (d, $J = 6.6$ Hz, 1H), 5.58 (m, 1H), 5.37 (m, 1H), 4.48–4.27 (m, 3H), 2.14 (s, 3H), 2.10 (s, 3H), 2.06 (s, 3H); MS (m/z) 385.14 [$\text{M} + \text{H}$] $^+$.

2.2.6. 2',3',5'-Tri-O-propionyl-acadesine (ZHM-03)

To the mixed solution of AICAR (1 g, 0.037 mol) and anhydrous pyridine (10 mL) was added propionic anhydride (1.94 mL). The reaction mixture was stirred 6 h at room temperature. The solution was quenched with EtOH (0.5 mL) and then concentrated three times *in vacuo* with 10 mL of toluene. The obtained white solid was collected, washed with cold EtOH (4 °C, 10 mL), concentrated *in vacuo*, and purified by column chromatography (ethyl acetate-petroleum ether, 1:2) to obtain ZHM-03. Yield: 70.3%; ^1H NMR (400 MHz, DMSO d_6) δ_{H} 7.78 (s, 1H), 6.95 (s, 2H), 6.51 (s, 2H), 5.95 (d, $J = 5.3$ Hz, 1H), 5.61 (t, $J = 5.6$ Hz, 1H), 5.40 (t, $J = 5.4$ Hz, 1H), 4.39 (m, 3H), 2.45–2.25 (m, 6H), 1.07–0.99 (m, 9H); MS (m/z): 449.17 [$\text{M} + \text{Na}$] $^+$.

2.2.7. 2',3'-O-(3-Methoxy-benzylidene)-acadesine (ZHM-04)

To the mixed solution of AICAR (5.0 g, 0.0194 mol) and ZnCl_2 (10.0 g) was added dry THF (10 mL) and 3-methoxybenzaldehyde (20 mL). The reaction mixture was stirred 2 days at room temperature. The solution was precipitated with diethyl ether (100 mL) and then filtered. The combined organic layers were washed with H_2O followed by saturated diethyl ether, filtered, and dried to obtain ZHM-04. Yield: 33.3%; ^1H NMR (400 MHz, DMSO d_6) δ_{H} 7.30 (s, 2H), 7.11–6.90 (m, 4H), 6.8–6.7 (m, 1H), 6.29 (dd, $J = 4.9, 3.0$ Hz, 1H), 5.91 (s, 2H), 5.79 (s, 1H), 5.53–5.48 (m, 1H),

5.09 (d, $J = 6.3$ Hz, 1H), 4.37 (t, $J = 3.8$ Hz, 2H), 3.79 (s, 3H), 3.65–3.53 (m, 2H); MS (m/z) 368.37 [$\text{M} + \text{H}$] $^+$.

2.2.8. 2',3'-O-(3-Fluoro-benzylidene)-acadesine (ZHM-05)

To the mixed solution of AICAR (5.0 g, 0.0194 mol) and ZnCl_2 (10.0 g) was added dry THF (10 mL) and 3-fluorobenzaldehyde (20 mL). The reaction mixture was stirred 2 days at room temperature. The solution was precipitated with diethyl ether (100 mL) and then filtered. The combined organic layers were washed with H_2O followed by saturated diethyl ether, filtered, and dried to obtain ZHM-05. Yield: 20.2%; ^1H NMR (400 MHz, DMSO d_6) δ_{H} 7.30 (s, 2H), 7.11–6.90 (m, 4H), 6.8–6.7 (m, 1H), 6.29 (dd, $J = 4.9, 3.0$ Hz, 1H), 5.91 (s, 2H), 5.79 (s, 1H), 5.53–5.48 (m, 1H), 5.09 (d, $J = 6.3$ Hz, 1H), 4.37 (t, $J = 3.8$ Hz, 2H), 3.65–3.53 (m, 2H); MS (m/z) 365.43 [$\text{M} + \text{H}$] $^+$.

2.2.9. 2',3'-O-(3-Chloro-benzylidene)-acadesine (ZHM-06)

To the mixed solution of AICAR (5.0 g, 0.0194 mol) and ZnCl_2 (10.0 g) was added dry THF (10 mL) and 3-chlorobenzaldehyde (20 mL). The reaction mixture was stirred 2 days at room temperature. The solution was precipitated with diethyl ether (100 mL) and then filtered. The combined organic layers were washed with H_2O followed by saturated diethyl ether, filtered, and dried to obtain ZHM-06. Yield: 34.6%; ^1H NMR (400 MHz, DMSO d_6) δ_{H} 7.30 (s, 2H), 7.11–6.90 (m, 4H), 6.8–6.7 (m, 1H), 6.29 (dd, $J = 4.9, 3.0$ Hz, 1H), 5.91 (s, 2H), 5.79 (s, 1H), 5.53–5.48 (m, 1H), 5.09 (d, $J = 6.3$ Hz, 1H), 4.37 (t, $J = 3.8$ Hz, 2H), 3.65–3.53 (m, 2H); MS (m/z) 381.30 [$\text{M} + \text{H}$] $^+$.

2.3. Animal experiments

Five-week-old male Kunming (KM) mice, weighing 18–22 g each, were purchased from the Beijing Experimental Animal Center (Beijing, China; Permit number: SCXK (Jing) 2019-0010). The operational procedures were carried out in accordance with the standards established in the Guide for the Care and Use of Laboratory Animals published by the Institute of Laboratory Animal Resources of the National Research Council (USA). This study was approved by the Animal Care and Use Committee of the Beijing Institute of Pharmacology and Toxicology. Best efforts were made to minimize the number of animals used and their suffering.

2.4. In-vivo anti-fatigue evaluation

2.4.1. Running wheel test

Male KM mice were divided randomly into eight groups ($n = 8$ for each group) and treated by intraperitoneal injection as follows: the blank control group (0.9% sodium chloride, 0.1 mL/mouse), AICAR group (0.0196 mmol/kg), and synthetic compound groups (ZHM-01 to ZHM-06, 0.0196 mmol/kg).

The test was performed on a JY-YLS-10B mouse running wheel instrument (Shilian Boyan, Beijing, China). Their exhaustion running distance was assessed after the following procedure: 16 rpm for 15 min, 18 rpm for 5 min, 20 rpm for 5 min, and 22 rpm for 5 min as an adaptive course before the test, and then 24 rpm was used until exhaustion. Mice that

rested more than four times (30 s) within 60 min indicated that they had reached exhaustion (Munteanu et al., 2018).

2.4.2. Weight-loaded swimming test

Male KM mice randomly divided and administered similar to that of running wheel test (the blank control group, AICAR group, and synthetic compound groups) were used for a weight-loaded swimming test.

The weight-loaded swimming test was conducted according to the previously described method with some modifications (Liu et al., 2018). The mice were loaded with a tin wire (6% of body weight) on their tail root and placed individually in a swimming pool (25 °C). The mice were determined to be exhausted when they failed to rise to the surface of the water to breathe within a 7 s period.

2.4.3. Hanging wire test

Male KM mice were divided randomly into three groups ($n = 8$ for each group) and treated by intraperitoneal injection as follows: the blank control group (0.9% sodium chloride, 0.1 mL/mouse), AICAR group (0.0196 mmol/kg), optimal compound group (ZHM-01, 0.0196 mmol/kg).

For this test, a thin line on two iron frames was hung, and the mice were placed on the thin line. The endurance of the mice was characterized by observing the time that their front and rear limbs held the thread. The times of the mice falling from the thin line were recorded.

2.4.4. Tail suspension test

Male KM mice randomly divided and administered similar to that of hanging wire test (the blank control group, AICAR group, and optimal compound group) were used for a tail suspension test.

For the tail suspension test, the mice were placed in a general soundproof behavior box, they were hung upside down, and their tails were stuck with adhesive tape about 1 cm from their tips. The endurance of the mice was characterized by observing their struggling time. The mice that did not struggle for more than 15 s were considered exhausted (Zhang et al., 2019a).

2.5. Open-field test

Male KM mice were divided randomly into two groups ($n = 8$ for each group) and treated by intraperitoneal injection as follows: the blank control group (0.9% sodium chloride, 0.1 mL/mouse) and the optimal compound group (ZHM-01, 0.0196 mmol/kg).

The open field test was used to evaluate the locomotor activity of mice. The test was carried out as the previously reported and make some modifications (Yang et al., 2018). The open field test was carried out in a quiet environment. The mice were placed in the center of a closed plane area of a closed box, which was divided into blocks, and their activities were measured by calculating the number of blocks passed within 10 min. The movements of the animals were recorded by a camera. The track tracing method was used to automatically count the total track distances of the mice under infrared light. This experiment was performed at 0.5 h and 3 h after administration, respectively.

2.6. Tissue collection and biochemical index

Blood samples were collected by retro-orbital puncture into EDTA capillary tubes for hematological and biochemical studies after the last bout of exercise. The mice were then sacrificed by cervical dislocation. The gastrocnemius of both hind legs was isolated, frozen, and stored at -80 °C until further analysis. The LA and BUN levels in the blood were determined by the corresponding kits.

2.7. Western blot analysis

The cells were washed with cold phosphate-buffered saline (PBS), then incubated with radioimmunoprecipitation (RIPA) lysis buffer for 15 min, and centrifuged at 1000g and 4 °C for 8 min. A bicinchoninic acid (BCA) assay kit was used to measure the protein concentration. Equal amounts of sample proteins were separated by sodium dodecyl sulfate-polyacrylamide gel electrophoresis (SDS-PAGE) to analyze the proteins, which were compared with a protein marker (CWBIO, Beijing, China). The proteins were transferred to a polyvinylidene fluoride membrane, and the membrane was blocked with 5% skimmed milk powder in tris-buffered saline containing Tween 20 (TBST) for 1 h. After washing with TBST three times, the membrane was incubated in a solution containing primary antibody (AMPK, p-AMPK, PGC-1 α , and GAPDH antibody, respectively) overnight at room temperature and visualized with horseradish peroxidase-coupled secondary antibody. Then, the protein bands were detected using an enhanced chemiluminescence kit (CWBIO, Beijing, China). An enhanced chemiluminescence western blot substrate (Pierce Biotechnology) was used to perform the immunodetection, which was detected with the ChemiDoc™ MP Imaging System (Bio-Rad, USA). The bands were analyzed by densitometric analysis with Image J software.

2.8. Cell culture and treatment

C2C12 myoblasts were cultured in DMEM containing 10% fetal bovine serum at 37 °C and 5% CO₂. The C2C12 cells were induced to undergo myogenic differentiation with a differentiation medium containing 2% horse serum for 6 days. Then cells were treated with 20 μ M ZHM-01 or the solvent dimethyl sulfoxide.

2.9. Safety test

Male KM mice were randomly divided into four groups ($n = 8$ for each group). And treated by intraperitoneal injection ZHM-01 as follows: normal dose group (0.0196 mmol/kg), 3-fold dose group (0.0588 mmol/kg), 10-fold dose group (0.196 mmol/kg) and 30-fold dose group (0.588 mmol/kg). The animals were observed to detect the changes of general behavior, poisoning symptoms, and mortality within 72 h.

Male KM mice were divided randomly into two groups ($n = 8$ for each group) and treated by intraperitoneal injection for 21 days as follows: the blank control group (0.9% sodium chloride, 0.1 mL/mouse) and the optimal compound group (ZHM-01, 0.0196 mmol/kg/day). The mice were then sacrificed by cervical dislocation, and the heart, liver, spleen, lung, and

kidney were collected and stained with hematoxylin and eosin for observation.

2.10. Statistical analysis

All the experimental data were expressed as mean \pm standard deviation. Significant differences were calculated by a two-tailed Student's *t*-test, and a *p*-value < 0.05 was considered to be statistically significant.

3. Results and discussion

3.1. Synthesis

In total, six AICAR derivatives (**ZHM-01** to **ZHM-06**, Scheme 1) were synthesized, and the structures of the intermediates and target compounds were confirmed by ^1H -nuclear magnetic resonance spectroscopy and mass spectrometry. Besides, the Log P value of AICAR was calculated by Chem-Draw software to be -3.28 , reflecting excessive hydrophilicity that is not conducive for druggability. Relatively, the Log P values of **ZHM-01** to **ZHM-06** were -1.92 , -2.59 , -0.63 , -0.75 , -0.47 , and -0.07 , respectively, indicating that these derivatives had an improved lipophilicity compared to that of AICAR.

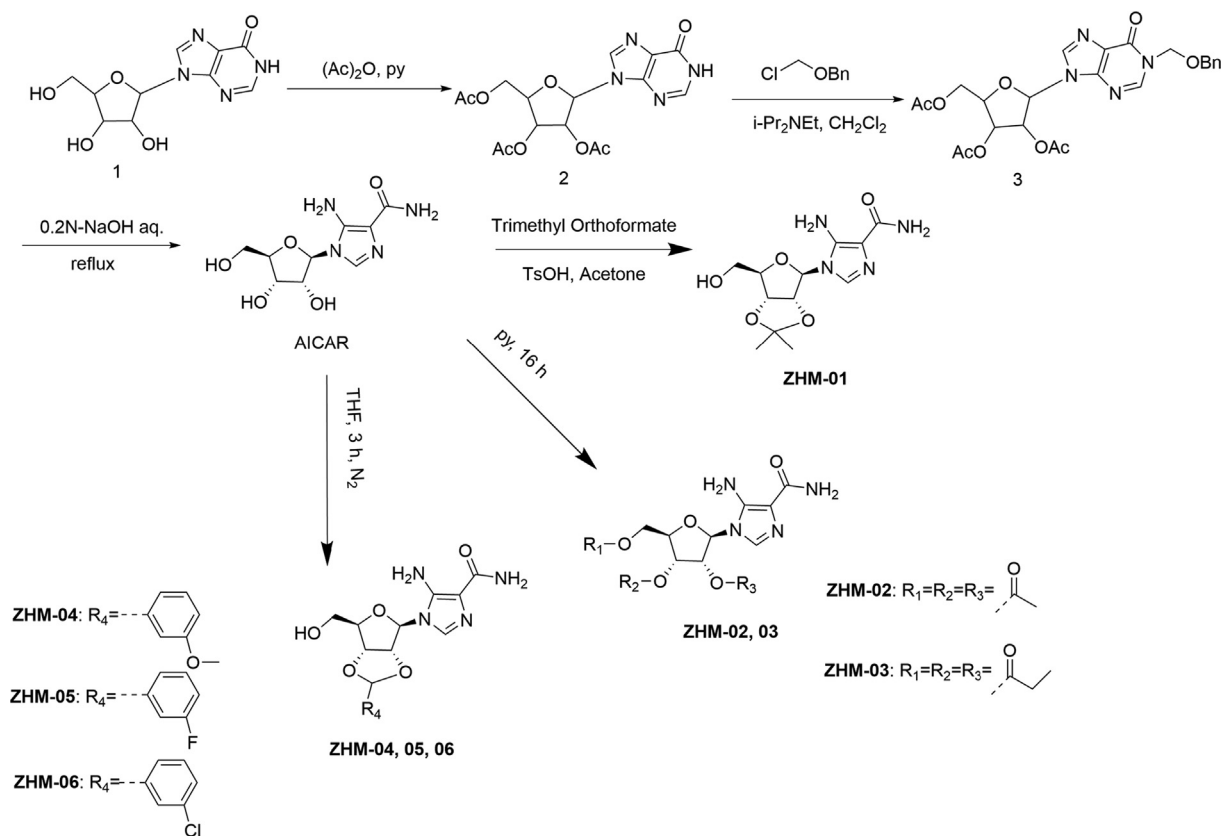
3.2. In-vivo anti-fatigue test

The running wheel test and the weight-loaded swimming test are widely used as animal models for anti-fatigue evaluation. The exhaustion level is related to the anti-fatigue efficiency.

As shown in Fig. 1A, the exhaustion distances of the running wheel test in the groups given **ZHM-01** (3627.2 m), **ZHM-02** (1942.5 m), **ZHM-03** (1521.3 m), **ZHM-04** (1647.2 m), **ZHM-05** (1170.4 m), **ZHM-06** (1462.4 m), and AICAR (1357.9 m), respectively, were greater than that of the blank control group (420.5 m, $P < 0.05$), indicating a clear anti-fatigue effect. The average exhaustion distance of the best compound, **ZHM-01**, was 8.6-fold and 2.7-fold greater than that of the blank control group and the AICAR group ($P < 0.05$).

The results of the weight-loaded swimming test (Fig. 1B) also demonstrated prolonged swimming times for all the mice treated with the AICAR derivatives or AICAR compared to that of the control group ($P < 0.05$). **ZHM-01** also showed the best enhancement of exercise endurance (51.1 min), which was 5.1-fold and 1.7-fold greater than those of the blank control group (10.0 min) and the AICAR group (30.0 min, $P < 0.05$).

In terms of the molecular structure, although substitution at the 2', 3', and 5'-hydroxy sites (**ZHM-02** and **ZHM-03**) or cyclization with the 2'- and 3'-hydroxyl groups with aro-



Scheme 1 Synthesis of AICAR derivatives.

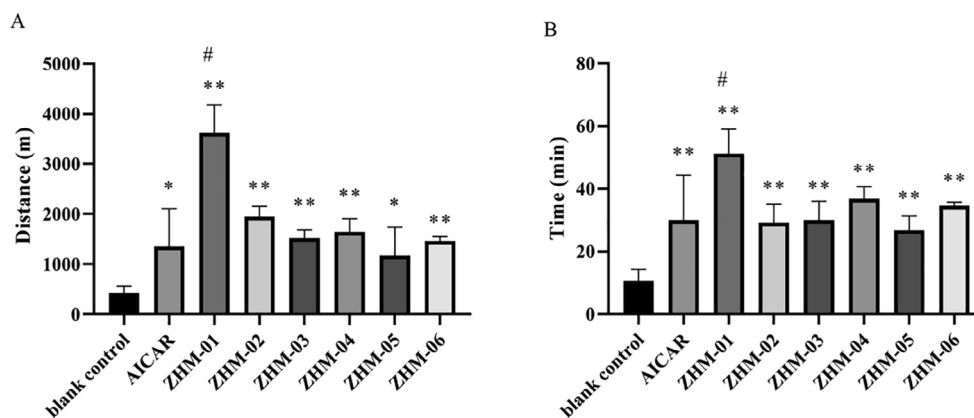


Fig. 1 Exhaustion distance in the running wheel test (A) and exhaustion time in the weight-loaded swimming test (B). * $P < 0.05$, ** $P < 0.01$ vs the blank control group; # $P < 0.05$, ## $P < 0.01$ vs the AICAR group. Data are presented as the mean \pm SD ($n = 8$).

matic substitution (ZHM-04 to ZHM-06) resulted in compounds with improved lipophilicity compared to that of AICAR, these derivatives did not show significantly greater anti-fatigue effects than AICAR ($P > 0.05$). However, cyclization of the 2'- and 3'-hydroxyl groups with an isopropylidene substitution resulted in a great improvement in the anti-fatigue effects compared to AICAR; therefore, ZHM-01 was chosen as the optimal molecule for further study.

The hanging wire test reflects the degree of grip endurance of the mouse limbs as well as their motor coordination capability. The results shown in Fig. 2A demonstrate that the suspension time of the ZHM-01 group was 2.8-fold greater than that of the AICAR group ($P < 0.05$) and 5.4-fold greater than that of the blank control group. The tail suspension test reflects the escape-related behavior while the mice were subjected to short-term inescapable stress (suspended by their tail) (Wang et al., 2021). The results depicted in Fig. 2B indicate no significant difference between the AICAR group and the blank control group, but the mice administered with ZHM-01 had a significantly prolonged struggle time compared with those of the AICAR group and the blank control group ($P < 0.05$).

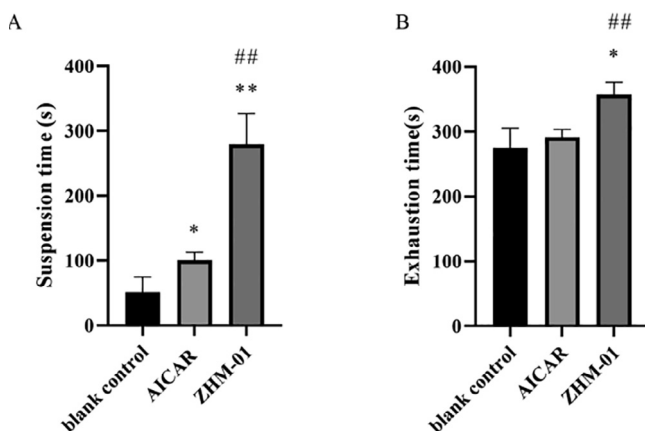


Fig. 2 Mean exhaustion time of mice in the hanging wire (A) and tail suspension (B) tests. * $P < 0.05$, ** $P < 0.01$ vs the blank control group; # $P < 0.05$, ## $P < 0.01$ vs the AICAR group. Data are shown as the mean \pm SD ($n = 8$).

AICAR was proved with definite endurance enhancing effect (Narkar et al., 2008), and has been regarded as a potential anti-fatigue drug or exercise mimic in many works (Handschin 2016, Manio et al., 2016). In our study, ZHM-01 treatment did show higher positive effects on the physiological endurance of mice than that of AICAR, indicating its significant potential to delay exercise-induced fatigue. To the best of our knowledge, ZHM-01 is one of the most potent anti-fatigue agents reported to date. Moreover, the anti-fatigue effects of AICAR were always tested after more than three week's administration, however, in our conditions, both the AICAR and ZHM-01 performed efficiency after single dosage.

3.3. ZHM-01 reduced LA and BUN accumulation

The LA level is always used to reflect the severity of fatigue. In our test, the LA content in the blank control group after exercise was greater than that of the sedentary control group (Fig. 3A), in line with general principles. The accumulation of LA in the AICAR group was even greater than that of the blank control group, while the mice ran the same running distance. This finding can be ascribed to the inherent side effect of AICAR, as previously reported (Scudiero et al., 2016). However, the LA level of the ZHM-01 group was significantly less than those of the blank control group and the AICAR group ($P < 0.05$), indicating that the mice in the ZHM-01 group were in a lower state of fatigue. In addition, this result also indicates that ZHM-01 reduced the side effect of LA accumulation compared to AICAR. As indicated in many works, LA is the product of anaerobic glycolysis during exercise, and the accumulation of LA in muscle leads to acidosis, which can interfere with the excitation-contraction coupling of human skeletal muscle, causing fatigue (Brooks 2020). The low LA level in ZHM-01 group was beneficial to prolong exercise endurance.

The BUN content is also an important biochemical index used to measure the level of exhaustion. The BUN content in the blank control group was significantly greater than that of the sedentary control group, while the AICAR and ZHM-01 groups had significantly lower BUN levels compared to that of the blank control group when at the same running distance ($P < 0.05$) (Fig. 3B). When catabolism of sugar and fat cannot fulfill the energy requirement after an intense and long period

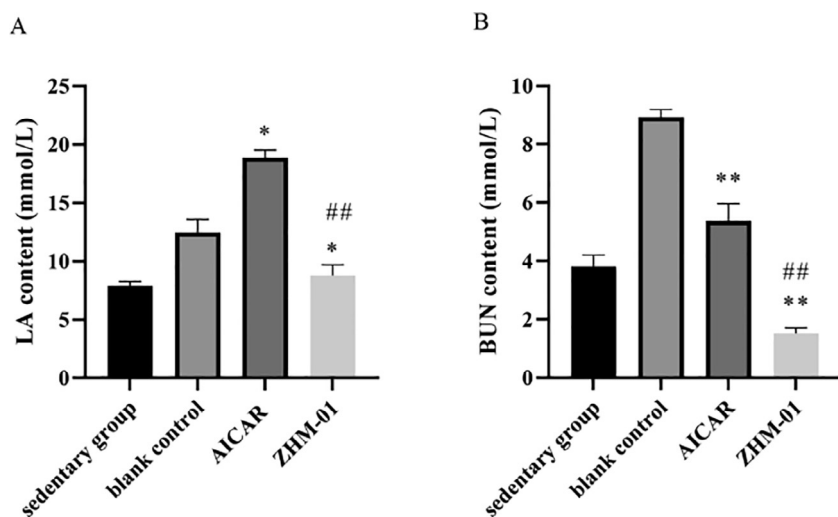


Fig. 3 Effect of **ZHM-01** on the contents of (A) lactic acid (LA) and (B) blood urea nitrogen (BUN) in mice. * $P < 0.05$, ** $P < 0.01$ vs the blank control group; # $P < 0.05$, ## $P < 0.01$ vs the AICAR group. Data are presented as the mean \pm SD ($n = 8$).

of exercise, catabolism of proteins, amino acids, and nucleotides will be strengthened to supply energy. Urea, produced as a result of protein metabolism, causes a significant increase in the serum nitrogen levels, which can in turn reduce the endurance and lead to fatigue (Chen et al., 2021; Zhu et al., 2021a). The lower BUN level of **ZHM-01** group than AICAR group after exercise could postpone muscle fatigue, which is in consistent with the trend of our behavioral test results.

The metabolite accumulation is usually considered as important factors causing exercise fatigue (Peng et al., 2021; Zhu et al., 2021a). These results provide further elucidation of the anti-fatigue mechanism of **ZHM-01**.

3.4. **ZHM-01** did not excite the central nervous system

As reported, the anti-fatigue effect can also be achieved by exciting the central nervous system. Several central nervous system excitatory drugs, including amphetamine, caffeine, ephedrine, modafinil, etc., have been shown in clinical studies to relieve fatigue and maintain wakefulness (Wesensten et al., 2004, Zhou et al., 2009). To evaluate whether **ZHM-01** exerts anti-fatigue effect by exciting the central nervous system, open-field tests were carried out at 0.5 h and 3 h after **ZHM-01** administration (Guo et al., 2015; Yang et al., 2018). The total trajectory distance of mice in the **ZHM-01** group and the blank control group showed no significant difference between each other at both time points (Fig. 4), indicating that **ZHM-01** did not increase locomotor activity. As a result, the anti-fatigue mechanism of **ZHM-01** does not involve central nervous system excitation.

3.5. **ZHM-01** enhanced the phosphorylation of AMPK

AMPK activity is related to increasing fatty acid oxidation and glucose uptake as well as mitochondrial biogenesis. Many literature reports have demonstrated that activation of AMPK can significantly improve the energy supply mode of skeletal muscle by accelerating the catabolic capacity and inhibiting the anabolism of energy consumption. Furthermore, the

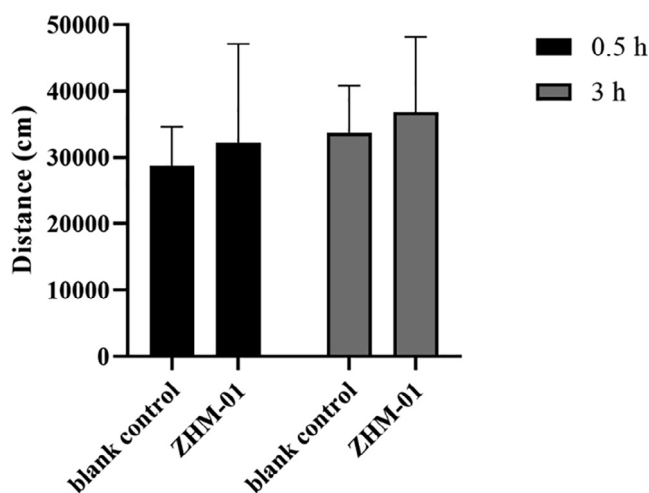


Fig. 4 Trajectory distances of mice in the open-field test. Data are expressed as the mean \pm SD ($n = 8$).

energy supply of skeletal muscle can be guaranteed, and exercise endurance can be effectively increased (Narkar et al., 2008). To test the effect of **ZHM-01** on the AMPK/PGC-1 α signaling pathway, western blot analysis was carried out using C2C12 cells. Phosphorylation of AMPK (p-AMPK) indicates the state of AMPK activation (Norikura et al., 2020). **ZHM-01** treatment upregulated p-AMPK compared with that of the AICAR group (Fig. 5A), and the p-AMPK/AMPK ratio of the **ZHM-01** group was greater than those of the AICAR group and the blank control group (Fig. 5B). Furthermore, the expression of PGC-1 α , which is downstream of AMPK, was also enhanced in our experiment. **ZHM-01** pharmacologically activating AMPK has potential to trigger many of the posttranslational and transcriptional adaptations to endurance training, collectively resulting in mice with a higher endurance capacity. Further research should be conducted to detect whether the **ZHM-01** modulates AMPK with selectivity and specificity.

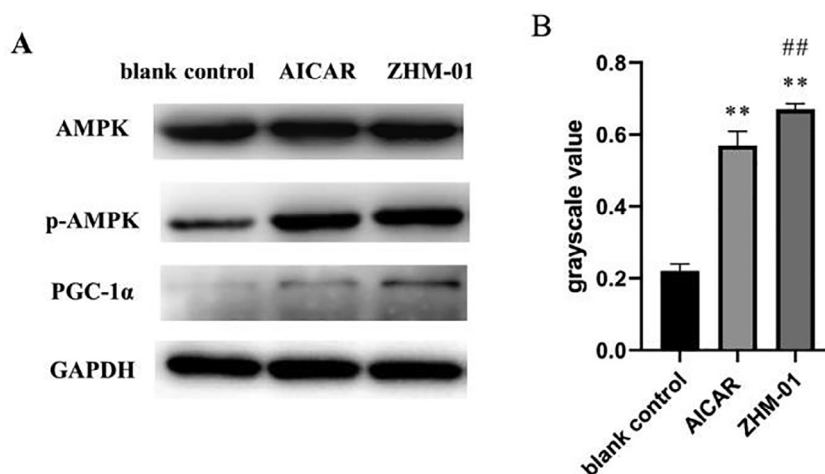


Fig. 5 (A) Western blot results for AMPK, phosphorylated (p)-AMPK, and PGC-1 α ; (B) the p-AMPK/AMPK ratio. * $P < 0.05$, ** $P < 0.01$ vs the blank control group; # $P < 0.05$, ## $P < 0.01$ vs the AICAR group.

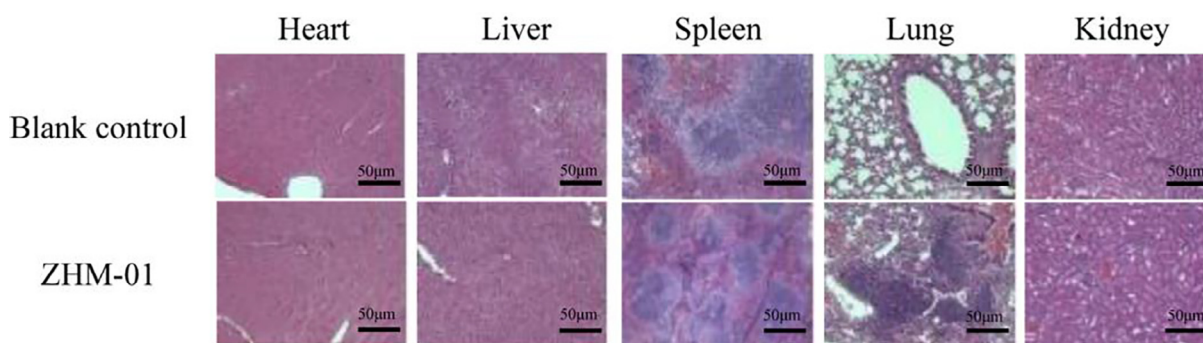


Fig. 6 Hematoxylin and eosin-stained histological sections of the heart, liver, spleen, lung, and kidneys at 21 days after mice were treated with **ZHM-01** (0.0196 mmol/kg/day) or 0.9% sodium chloride (blank control). The images were obtained using a Leica microscope. Magnification, 400 \times . Scale bar = 50 μ m.

3.6. Safety of ZHM-01

ZHM-01 showed no acute toxicity at doses of 0.588 mmol/kg (30-fold higher than that in the functional tests), 0.196 mmol/kg (10-fold), and 0.0588 mmol/kg (3-fold), separately. No death or sign of toxicity was recorded during the 72-h observation period.

The safety of **ZHM-01** was also evaluated at three weeks after mice were intraperitoneally injected daily with **ZHM-01** a dosage of 0.0196 mmol/kg. There were no obvious abnormalities in the spirit, feeding, drinking, breathing, death, hair, feces, or movement of the mice. In addition, tissue sections of the sampled heart, liver, spleen, lung, and kidney were observed by hematoxylin and eosin staining, and no obvious inflammation or substantial damage was found (Fig. 6). These results demonstrate the good biological safety of **ZHM-01** *in vivo*.

4. Conclusion

In conclusion, six AICAR derivatives with modification at the hydroxyl sites of ribose were synthesized and evaluated their anti-fatigue

properties. The optimal compound **ZHM-01**, typical of cyclization by the 2'- and 3'-hydroxyl groups with an isopropylidene substitution, resulted in a great improvement in the anti-fatigue effects compared to AICAR. The mechanism related to decreasing LA and BUN accumulation, as well as enhancing AMPK/PGC-1 α pathway. To our knowledge, **ZHM-01** is one of the most effective anti-fatigue agents reported so far. **ZHM-01** exhibited appealing potential for development and utilization as a novel anti-fatigue drug, which may offer a new therapeutic approach for fatigue-related diseases and sub-health.

Declaration of interest

The authors confirm that they have no conflicts of interest with respect to the work described in this manuscript.

Acknowledgement

This work was supported by grants from Beijing Natural Science Foundation (7202146), and National Key Research and Development Project of China (2020YFC1712702).

Contributors

L.X., X.L. and W.S. contributed to the conception of the study; H.Z. and W.Z. performed the experiment; L.X., H.Z. and W.Z. contributed significantly to analysis and article preparation; L.X., H.Z. and T.Z. performed the data analysis and wrote the article; X.D. and A.Z. helped perform the analysis with constructive discussions. All the authors have read the article and agree to its contents.

References

- Brooks, G.A., 2020. Lactate as a fulcrum of metabolism. *Redox Biol.* 35,. <https://doi.org/10.1016/j.redox.2020.101454> 101454.
- Chen, Y.J., Kuo, C.Y., Kong, Z.L., et al, 2021. Anti-Fatigue Effect of a Dietary Supplement from the Fermented By-Products of Taiwan Tilapia Aquatic Waste and *Monostroma nitidum* Oligosaccharide Complex. *Nutrients* 13, 1688. <https://doi.org/10.3390/nu13051688>.
- Coqueiro, A.Y., Rogero, M.M., Tirapegui, J., 2019. Glutamine as an Anti-Fatigue Amino Acid in Sports Nutrition. *Nutrients* 11, 863. <https://doi.org/10.3390/nu11040863>.
- Cui, J., Xia, P., Zhang, L., et al, 2020. A novel fermented soybean, inoculated with selected *Bacillus*, *Lactobacillus* and *Hansenula* strains, showed strong antioxidant and anti-fatigue potential activity. *Food Chem.* 333,. <https://doi.org/10.1016/j.foodchem.2020.127527>.
- D'Errico, S., Oliviero, G., Borbone, N., et al, 2012. A facile synthesis of 5'-fluoro-5'-deoxyacadesine (5'-F-AICAR): a novel non-phosphorylatable AICAR analogue. *Molecules (Basel, Switzerland)* 17, 13036–13044. <https://doi.org/10.3390/molecules171113036>.
- Dixon, R., Gourzis, J., McDermott, D., et al, 1991. AICA-riboside: safety, tolerance, and pharmacokinetics of a novel adenosine-regulating agent. *J. Clin. Pharmacol.* 31, 342–347. <https://doi.org/10.1002/j.1552-4604.1991.tb03715.x>.
- Gao, H., Zhang, W., Wang, B., et al, 2018. Purification, characterization and anti-fatigue activity of polysaccharide fractions from okra (*Abelmoschus esculentus* (L.) Moench). *Food Funct.* 9, 1088–1101. <https://doi.org/10.1039/c7fo01821e>.
- Guo, K, Zhu, J, Quan, X, et al, 2015. Comparison of the effects of pretreatment with repeated electroacupuncture at GV20 and ST36 on fatigue in rats. *Acupunct Med.* 33, 406–412. <https://doi.org/10.1136/acupmed-2014-010686>.
- Handschin, C., 2016. Caloric restriction and exercise “mimetics”: Ready for prime time? *Pharmacol. Res.* 103, 158–166. <https://doi.org/10.1016/j.phrs.2015.11.009>.
- Hu, M., Du, J., Du, L., et al, 2020. Anti-fatigue activity of purified anthocyanins prepared from purple passion fruit (*P. edulis* Sim) epicarp in mice. *J. Funct. Foods* 65,. <https://doi.org/10.1016/j.jff.2019.103725> 103725.
- Kim, J., Beak, S., Ahn, S., et al, 2022. Effects of taurine and ginseng extracts on energy metabolism during exercise and their anti-fatigue properties in mice. *Nutrit. Res. Pract.* 16, 33–45. <https://doi.org/10.4162/nrp.2022.16.1.33>.
- Li, M., Tian, X., Li, X., et al, 2021. Anti-fatigue activity of gardenia yellow pigment and Cistanche phenylethanol glycosides mixture in hypoxia. *Food Biosci.* 40,. <https://doi.org/10.1016/j.fbio.2021.100902> 100902.
- Lin, S.C., Hardie, D.G., 2018. AMPK: Sensing Glucose as well as Cellular Energy Status. *Cell Metab.* 27, 299–313. <https://doi.org/10.1016/j.cmet.2017.10.009>.
- Liu, R., Wu, L., Du, Q., et al, 2018. Small Molecule Oligopeptides Isolated from Walnut (*Juglans regia* L.) and Their Anti-Fatigue Effects in Mice. *Molecules (Basel Switzerland)* 24, 45. <https://doi.org/10.3390/molecules24010045>.
- Luo, C., Xu, X., Wei, X., et al, 2019. Natural medicines for the treatment of fatigue: Bioactive components, pharmacology, and mechanisms. *Pharmacol. Res.* 148,. <https://doi.org/10.1016/j.phrs.2019.104409> 104409.
- Manio, M.C., Inoue, K., Fujitani, M., et al, 2016. Combined pharmacological activation of AMPK and PPAR δ potentiates the effects of exercise in trained mice. *Physiol. Rep.* 4, e12625.
- Munteanu, C., Rosioru, C., Tarba, C., et al, 2018. Long-term consumption of energy drinks induces biochemical and ultrastructural alterations in the heart muscle. *Anatol. J. Cardiol.* 19, 326–323. <https://doi.org/10.14744/AnatolJCardiol.2018.90094>.
- Nakagawasai, O., Yamada, K., Sakuma, W., et al, 2021. A novel dipeptide derived from porcine liver hydrolysate induces recovery from physical fatigue in a mouse model. *J. Funct. Foods* 76,. <https://doi.org/10.1016/j.jff.2020.104312> 104312.
- Narkar, V.A., Downes, M., Yu, R.T., et al, 2008. AMPK and PPAR δ agonists are exercise mimetics. *Cell* 134, 405–415. <https://doi.org/10.1016/j.cell.2008.06.051>.
- Norikura, T., Kajiya, S., Sugawara, M., et al, 2020. cis-Banglene, a bangle (*Zingiber purpureum*)-derived bioactive compound, promotes mitochondrial biogenesis and glucose uptake by activating the IL-6/AMPK signaling pathway in C2C12 skeletal muscle cells. *J. Funct. Foods* 64,. <https://doi.org/10.1016/j.jff.2019.103632> 103632.
- Peng, F., Yin, H., Du, B., et al, 2021. Anti-fatigue activity of purified flavonoids prepared from chestnut (*Castanea mollissima*) flower. *J. Funct. Foods* 79,. <https://doi.org/10.1016/j.jff.2021.104365> 104365.
- Scudiero, O., Nigro, E., Monaco, M.L., et al, 2016. New synthetic AICAR derivatives with enhanced AMPK and ACC activation. *J. Enzyme Inhib. Med. Chem.* 31, 748–753. <https://doi.org/10.3109/14756366.2015.1063622>.
- Shimizu, T., Hoshino, H., Nishi, S., et al, 2010. Anti-fatigue effect of dicethiamine hydrochloride is likely associated with excellent absorbability and high transformability in tissues as a Vitamin B (1). *Eur. J. Pharmacol.* 635, 117–123. <https://doi.org/10.1016/j.ejphar.2010.02.053>.
- Tang, X., Zhuang, J., Chen, J., et al, 2011. Arctigenin efficiently enhanced sedentary mice treadmill endurance. *PLoS One* 6, e24224.
- Wang, P., Wang, D., Hu, J., et al, 2021. Natural bioactive peptides to beat exercise-induced fatigue: A review. *Food Biosci.* 43,. <https://doi.org/10.1016/j.fbio.2021.101298> 101298.
- Weihrauch, M., Handschin, C., 2018. Pharmacological targeting of exercise adaptations in skeletal muscle: Benefits and pitfalls. *Biochem. Pharmacol.* 147, 211–220. <https://doi.org/10.1016/j.bcp.2017.10.006>.
- Wesstenen, N.J., Belenky, G., Thorne, D.R., et al, 2004. Modafinil vs. caffeine: effects on fatigue during sleep deprivation. *Aviat. Space Environ. Med.* 75, 520–525.
- Wu, R.M., Sun, Y.Y., Zhou, T.T., et al, 2014. Arctigenin enhances swimming endurance of sedentary rats partially by regulation of antioxidant pathways. *Acta Pharmacol. Sin.* 35, 1274–1284. <https://doi.org/10.1038/aps.2014.70>.
- Xu, M., Liang, R., Li, Y., et al, 2017. Anti-fatigue effects of dietary nucleotides in mice. *Food Nutr. Res.* 61, 1334485. <https://doi.org/10.1080/16546628.2017.1334485>.
- Yang, Q.Y., Lai, X.D., Ouyang, J., et al, 2018. Effects of Ginsenoside Rg3 on fatigue resistance and SIRT1 in aged rats. *Toxicology* 409, 144–151. <https://doi.org/10.1016/j.tox.2018.08.010>.
- Yoon, K.J., Zhang, D., Kim, S.J., et al, 2019. Exercise-induced AMPK activation is involved in delay of skeletal muscle senescence. *Biochem. Biophys. Res. Commun.* 512, 604–610. <https://doi.org/10.1016/j.bbrc.2019.03.086>.
- Zhang, X., Jing, S., Lin, H., et al, 2019a. Anti-fatigue effect of anwulignan via the NRF2 and PGC-1 α signaling pathway in mice. *Food Funct.* 10, 7755–7766. <https://doi.org/10.1039/c9fo01182j>.

- Zhang, Y., Ryu, B., Cui, Y., et al, 2019b. A peptide isolated from *Hippocampus abdominalis* improves exercise performance and exerts anti-fatigue effects via AMPK/PGC-1 α pathway in mice. *J. Funct. Foods* 61,. <https://doi.org/10.1016/j.jff.2019.103489> 103489.
- Zheng, Y., Zhang, W.C., Wu, Z.Y., et al, 2019. Two macamide extracts relieve physical fatigue by attenuating muscle damage in mice. *J. Sci. Food Agric.* 99, 1405–1412. <https://doi.org/10.1002/jsfa.9318>.
- Zhou, Y., Zhu, Z.L., Guan, X.X., et al, 2009. Reciprocal roles between caffeine and estrogen on bone via differently regulating cAMP/PKA pathway: the possible mechanism for caffeine-induced osteoporosis in women and estrogen's antagonistic effects. *Med. Hypotheses* 73, 83–85. <https://doi.org/10.1016/j.mehy.2009.01.029>.
- Zhu, S., Yang, W., Lin, Y., et al, 2021a. Antioxidant and anti-fatigue activities of selenium-enriched peptides isolated from *Cardamine violifolia* protein hydrolysate. *J. Funct. Foods* 79,. <https://doi.org/10.1016/j.jff.2021.104412> 104412.
- Zhu, J., Yi, J., Kang, Q., et al, 2021b. Anti-fatigue activity of hemp leaves water extract and the related biochemical changes in mice. *Food Chem. Toxicol.* 150,. <https://doi.org/10.1016/j.fct.2021.112054> 112054.